Journal of the Serbian Chemical Society
JSCS-info@shd.org.rs • www.shd.org.rs/JSCS
J. Serb. Chem. Soc. 80 (2) 223–235 (2015)
JSCS–4712
UDC 677.52:678.742:541.124.2:548.3
Original scientific paper

The influence of glass fibers on the morphology of β-nucleated isotactic polypropylene evaluated by differential scanning calorimetry

ACO JANEVSKI[1]* and GORDANA BOGOEVA-GACEVA[2]

[1]*Faculty for Technology, "Goce Delcev" University, 2000 Stip, FYR Macedonia and* [2]*Faculty of Technology and Metallurgy, St. Cyril and Methodius University, 1000 Skopje, FYR Macedonia*

(Received 23 March, revised 26 May 2014, accepted 27 May 2014)

Abstract: The presence of fillers/fibers can significantly affect the polymorphic behavior of semi-crystalline polymers. The influence of glass fibers on morphology of β-nucleated isotactic polypropylene (iPP) during isothermal and nonisothermal crystallization was analyzed in detail by differential scanning calorimetry (DSC), and the kinetics and thermodynamic parameters were determined for the systems containing 10–60 % glass fibers. The presence of glass fibers in the model composites with β-iPP had an insignificant effect on the morphology of the polymer. Thermodynamic and kinetics parameters of crystallization of iPP in model composites were similar to those obtained for the nucleated polymer. The relative content of β-crystalline phase was slightly affected by increasing glass the fiber content from 10 to 60 mas. % due to appearance of α-crystallites. Moreover, the stability of the β-crystalline phase was decreased with increasing glass fiber content and there appeared a certain amount of β_1 and β_2 phases, which are known to be disposed to recrystallization.

Key words: crystallization; composites; DSC; polypropylene; β-nucleated.

INTRODUCTION

Isotactic polypropylene (iPP) is one of the most important commodity semi-crystalline thermoplastic widely used in many areas because of its versatility, good physical and mechanical properties, recyclability and low cost. iPP has been studied extensively for its polymorphic characteristics and crystallization behavior,[1–18] since the formation of specific crystalline forms (α, β and γ, or smectic) can affect the macroscopic behavior quite dramatically.[12–18] Commonly, under usual processing conditions, iPP crystallizes into the thermodynamically most stable monoclinic α-phase, which is responsible for its good

* Corresponding author. E-mail: aco.janevski@ugd.edu.mk
doi: 10.2298/JSC140324055J

strength and modulus. The trigonal β-form is metastable and can be obtained, or can become predominant, under specific crystallization conditions or in the presence of β-nucleating agents. β-Nucleated iPP exhibits large differences in mechanical properties as compared to the usual α-PP, namely higher toughness, ductility and drawability. The orthorhombic γ-form is the least frequently observed, and usually it can be obtained after crystallization at high pressures.[19–21]

The tailoring of polymorphic behavior of iPP, especially in composite materials where additional fiber-nucleating activity is observed,[4,7,22–27] seems to be important for the adjustment of the final properties of a material and the design of materials for certain applications. From a practical point of view, the addition of β-nucleating agents represents the most effective and accessible method to produce different levels of β-form iPP or even pure β-iPP. Among them, quinacridone pigment, pimelic acid/calcium stearate mixture, calcium salts of suberic or pimelic acid, calcium carbonate ($CaCO_3$) modified with dimeric aluminates, *N*,*N*-dicyclohexyl-terephthalamide and *N*,*N*-dicyclohexyl-2,6-naphthalene-dicarboxamide are reported in the literature.[11–14]

The properties of semi-crystalline polymers, used as matrices in composite materials are also related to the conditions during the processing cycle of heating (melting) and cooling (crystallization), since the morphology developed depends mostly on the time–temperature regime. For this reason, the differential canning calorimetry (DSC) method is often used for investigation of the behavior of filler/fiber–polymer composite materials in terms of crystalline structure and influencing parameters during isothermal or nonisothermal regimes.[24–28]

In a previous studies, the crystallization behavior and morphology of modified and unmodified iPP, used as a matrix in composites with differently sized/ /treated glass fibers, were thoroughly studied.[24–28] It was shown that glass fibers with a different surface chemistry exhibited different nucleating effects towards iPP, evaluated by crystallization parameters, but generally, they all acted as weak α-nucleators. In this work, the influence of glass fibers on the crystallization behavior, polymorphic composition and crystalline morphology of β-nucleated iPP was investigated.

EXPERIMENTAL

Commercial grade Shell homo-iPP with a weight-average molecular weight, $\bar{M}_w$, of 158,500 and a polydispersity index, $\bar{M}_w / \bar{M}_n$ of 6.36, as determined by gel permeation chromatography, GPC, was used. The concentrations of meso triads (0.94) and their average lengths (*n*) and probabilities for meso additions (0.96) were determined by ^{13}C-NMR spectroscopy. β-Nucleated iPP (BNP) was obtained by mixing 0.1 mas. % calcium pimelate with iPP in a Brabender mixer PL 2000 at 460 K. To study the influence of glass fibers (GF) on crystallization peculiarities and morphology of the polymer, model composites BNP/glass-fibers were prepared with 10, 20, 30, and 60 mas. % of GF (sized with thermoplastics compatible sizing). The abbreviations of model composites and their compositions are given in Table I.

TABLE I. Designation and content of the samples

Designation	Composition
BNP	iPP + 0.1 mass % Ca pimelate
C1BNPGF	BNP +10 mass % glass fiber
C2BNPGF	BNP + 20 mass % glass fiber
C3BNPGF	BNP + 30 mass % glass fiber
C6BNPGF	BNP + 60 mass % glass fiber
iPP	iPP Shell

Isothermal and nonisothermal crystallization of BNP was analyzed by DSC. In isothermal regime, the sample was rapidly heated to 478 K and held in the molten state for 5 min, to erase the thermal history of the polymer. Then the sample was cooled to a given crystallization temperature, T_c at a cooling rate of 80 K min^{-1}. Isothermal crystallization was realized at T_c until crystallization was completed. The crystallization under nonisothermal conditions was performed by cooling at different cooling rates: 1, 3, 5, 10, 15 and 20 K min^{-1}. The experiments were performed with a Perkin Elmer DSC-7 analyzer under nitrogen and indium and zinc were used for the calibration. The sample weight in all experiments was 7.0 mg. Based on the determined values for the enthalpy of crystallization, the extent of crystallization (crystal conversion), α, was calculated using Eq. (1):

$$\alpha = \frac{\int_0^t \left(\frac{\mathrm{d}H}{\mathrm{d}t}\right)\mathrm{d}t}{\int_0^\infty \left(\frac{\mathrm{d}H}{\mathrm{d}t}\right)\mathrm{d}t} = f(t) \quad (1)$$

From the obtained $\alpha = f(t)$ curves and the induction time (t_i), the half-time of crystallization ($t_{0.5}$) was determined.[28]

The amounts of α- and β-phase iPP in the model composites were calculated based on the corresponding melting enthalpies, $\Delta_{melt}H_\beta^0$ and $\Delta_{melt}H_\alpha^0$, using the following values: 193[29] and 209 J g^{-1},[30-32] respectively. The melting peaks of the both polymorphic phases appeared well resolved on the DSC thermograms, enabling the calculation of the amount of α- and β-phase iPP using Eqs. (2)–(4):[23,33]

$$X_\beta = \frac{\Delta_{melt}H_\beta}{\Delta_{melt}H_\beta^0} \quad (2)$$

$$X_\alpha = \frac{\Delta_{melt}H_\alpha}{\Delta_{melt}H_\alpha^0} \quad (3)$$

$$U_\beta = \frac{X_\beta}{(X_\alpha + X_\beta)} \quad (4)$$

where X_α and X_β are the amount of α- and β-phase, respectively, and U_β is the relative content of the β-phase in the overall crystalline structure of the sample.

Melt nucleation and crystallization of PPs were followed by polarizing light microscope (PLM, Leica, Biomed), equipped with a hot-stage device, temperature controller and photo camera.

The X-ray diffraction patterns were recorded on a Universal X-ray diffractometer with KCu$_\alpha$ radiation at 40 kV and 20 μA.

Theoretical background of the approach applied is given in the Supplementary material to this paper.

RESULTS AND DISCUSSION

Ca-pimelate is known as an efficient β nucleator for iPP.[34] The XRD-patterns of BNP obtained on addition of 0.1 mas. % calcium pimelate are presented in Fig. 1.

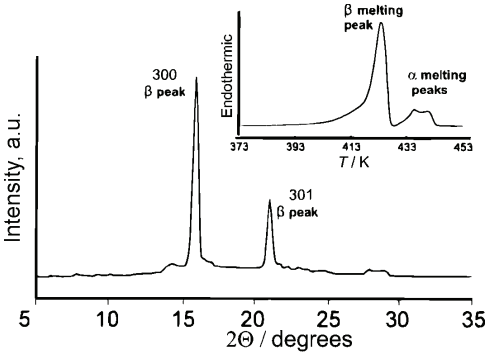

Fig. 1. X-Ray diffraction pattern and DSC melting thermogram (inset) of BNP.

Obviously, the dominant phase in this sample was the β-modification of iPP: the dominant peak at the diffraction angle 16.2° was attributed to the β (300) plane, while those of the α-modification (at 14.2, 17.0 and 18.4°, corresponding to the (110), (040) and (130) planes, respectively) were of weak intensity. Consistent with the results from XRD analysis, the melting DSC peak of the β crystallites (T_m = 424.2 K) was of high intensity, contrary to the one arising from the presence of α crystallites. The characteristic morphology of β-spherulites, originating after mixing iPP with Ca-pimelate, is also clearly illustrated in Fig. 2. The K_β parameter determined from the XRD-patterns by the Turner–Jones method[35] was 0.94, while the U_β-value calculated from the melting endotherm was 0.84 (Fig. 1, inset).

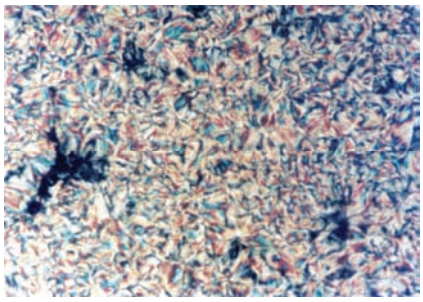

Fig. 2. Polarizing optical micrograph of BNP.

The isothermal crystallization of BNP and the composites were performed at temperatures from 388 to 409 K, the range, according to Hoffman,[36–39] known as

region III. The DSC melting curves of the isothermally crystallized samples at different T_c values are shown in Fig. 3. The melting peak temperature of the samples appeared at 418–428 K.

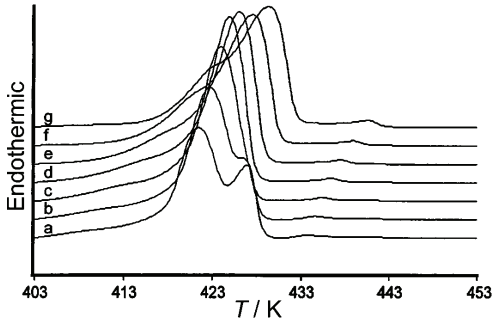

Figure 3. DSC melting thermograms of BNP after isothermal crystallization at different T_c values: a) 391; b) 394; c) 397; d) 400; e) 403; f) 406 K; g) 409 (heating rate 10 K min^{-1}).

Small endotherms, arising from the melting of α-crystallites present in the samples are seen along with the main peak of the β-crystallites (Fig. 3). The crystal structures β_1 and β_2[14] were registered during the melting of the samples crystallized at temperatures lower than 397 K. The DSC melting thermograms obtained after crystallization at T_c values higher than 397 K are used to determine the equilibrium melting temperature, T_m^0, applying the Hoffman–Weeks method,[40] and the results for BNP in comparison to iPP and GF-composites are presented in Table II.

Table II. Surface energies, σ_e, equilibrium melting temperatures, T_m, and the γ constants determined from isothermal DSC data

Parameter	BNP	C1BNPGF	C2BNPGF	C3BNPGF	C6BNPGF	iPP
T_m^0 / K	446.0	451.1	452.0	451.0	451.0	465.7
$\sigma_e \times 10^3$ / J m^{-2}	80.7	93.0	105.0	102.0	101.0	208
γ	2.20	1.84	1.81	1.86	1.87	2.37
θ	0.34	0.44	0.46	0.43	0.43	1.00

The determined value of 446 K for T_m^0 lies in the range of values previously published for β-iPP.[36,38]

The Avrami plots for BNP and the model BNP/glass fiber composites in the investigated region of crystallization temperatures, similarly to other β-nucleated systems,[42–44] were almost linear (Fig. 4), although two crystal phases with different energetic parameters were formed during the crystallization. Linearity of these plots enabled the determination of the overall kinetics parameters, which are not related to the certain crystalline phase but represent overall characteristic of the system as a whole (Table III).

In the Avrami equation, *n* may show values ranging from below 1 to far above 6. Any one value, whole or fractional, however, is not uniquely fixed to

any one set of conditions. Additional information on nucleation, morphology, and possibly even mechanism is necessary to interpret fully the exponent *n*. For many macromolecules, *n* is close to three and a picture of a thermal heterogeneous nucleation followed by spherulitic growth is acceptable; others require = *n* = 4, indicative of thermal nucleation, which is most often thermal heterogeneous nucleation followed by spherulitic growth. The also frequently observed exponent *n* = 2 could well be related to fibrillar or lamellar crystal growth following thermal or athermal nucleation. The Avrami index *n* is composed of both a geometric index *n** and a nucleation index *m*. The latter may have a wide range of values, depending on the nature of the nucleation process. This comprehension provides a basis to understand better the many non-integer values of *n* occurring in the literature, as well as values that are greater than 4.[42]

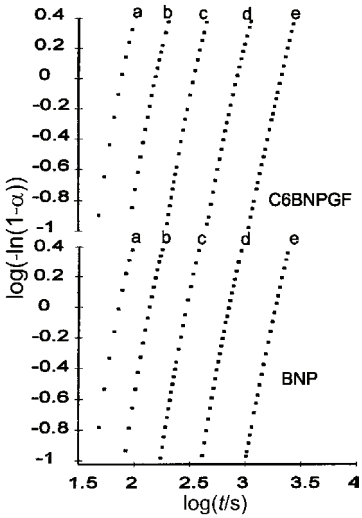

Fig. 4. Avrami plots for BNP and C6BNPGF at different T_c values: a) 397; b) 400; c) 403; d) 406; e) 409 K.

Table III. Avrami index, *n*, and the overall kinetic constant, *k*, at different T_c values

T_c / K	BNP		C1BNPGF		C2BNPGF		C3BNPGF		C6BNPGF	
	n	k / 10^{-10} s^{-n}	*n*	k / 10^{-10} s^{-n}	*n*	k / 10^{-10} s^{-n}	*n*	k / 10^{-10} s^{-n}	*n*	k / 10^{-10} s^{-n}
397	3.9	600	3.8	650	4.1	130	4.3	130	4.0	220
400	3.9	32	3.9	34	3.9	21	3.9	30	3.7	65
403	3.9	1.9	3.8	2.2	3.7	2.8	3.7	4.8	3.7	4.4
406	3.8	0.16	3.8	0.089	3.5	0.67	3.4	1.3	3.4	1.2
409	3.5	0.026	3.8	0.085	3.1	0.74	3.3	0.15	3.3	0.078

The Avrami exponent, *n*, had values between 3.1 and 4.3, indicating that heterogeneous nucleation occurred and a tendency of decreasing *n* with increasing T_c was noticed, and it is more pronounced with increasing glass fiber content.

The exponent n ranging from 3.74 to 4.35 were determined for composite systems with β-nucleated iPP and talc-nucleated iPP.[41]

The results for T_m^0, σ_e, the γ-constant and the parameter θ for the model composites are summarized in Table II. As can be seen, the values of T_m^0 increased with increasing glass fiber content and they had values between those for β-nucleated iPP and iPP.

Generally, a good nucleating agent provides a surface that reduces the free energy barrier for primary nucleation. The low energy required implies a highly effective nucleating agent. The crystal fold surface energy (σ_e) for BNP, determined in this study was 80.7 mJ m^{-2}, which was similar to that found by Varga.[39] Generally, different values for σ_e are reported in the literature, mostly depending on the investigated region of crystallization. The σ_e obtained for region III (that, according to some authors, starts at 410 K[36] and to others at 406 K[37]) ranges from 85.4 to 48–67 mJ m^{-2}.[38,41] The value of 85.5 mJ m^{-2} was determined by Li *et. al* for β-nucleated iPP compared to 107, mJ m^{-2} for the neat polymer.[43] In the present model composite systems, the σ_e values increased with increasing content of glass fibers.

The curves of induction time for crystallization, t_i and the half-time of crystallization, $t_{0.5}$ versus supercooling are shown in Fig. 5. Obviously, the values of both t_i and $t_{0.5}$ determined for the GF-model composites are closer to those determined for BNP. A similar tendency was also found for the values of σ_e.

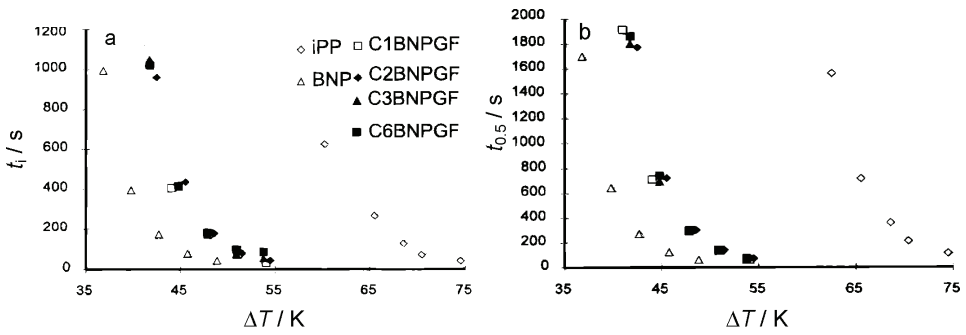

Fig. 5. Dependence of the induction time (a) and the half-time of crystallization (b) for iPP, BNP and the BNP/GF-composites on ΔT_c.

Based on the kinetics parameters and calculated value for T_m^0, the energy of the formation of a nucleus with critical dimensions was determined, and the results are shown in Fig. 6 as the ratio between the energy in a given system (BNP or composite sample) and the energy of a non-nucleated system. It could be concluded that favorable conditions for nucleation were attained in the nucleated polymer, whereas in the model composites with glass fibers, the nucleation

was slightly depressed. This finding was confirmed by the dependence of this factor (obtained for T_c = 409 K) on the content of glass fibers, as shown in Fig. 7.

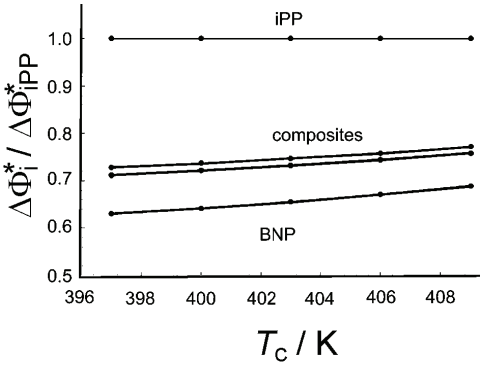

Fig. 6. Ratios of the energy of formation of nuclei of critical dimensions for iPP, BNP and the GF-composites *vs.* T_c.

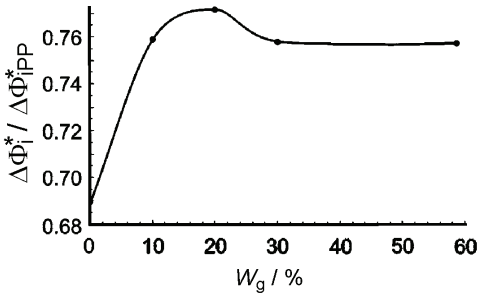

Fig. 7. Ratios of the energy of formation of nuclei of critical dimensions *vs.* the content of glass fibers (W_g / mas. %) at T_c = 409 K.

From the melting thermograms (melting performed after isothermal crystallization), the amounts of the α- and β-phase in the model composites were determined (Fig. 8). The amount of β-phase in iPP and C1BNPGF slightly increased with increasing T_c, while in composites with 20–60 mas. % glass fibers, it decreases at $T_c \geq 403$ K.

The content of α-phase, although low, increased with increasing T_c, while U_β decreased (Fig. 9), and this trend was most pronounced in the composite sample with 60 mas. % glass fibers.

As it is evident from Figs. 8 and 10, despite the high amount of glass fibers in the model composites, the relative content of the β-crystalline phase was over 0.85 for C6BNPGF and even higher for the composites with less than 60 mas. % glass fibers. It should be mentioned that a similar effect was found for PP/multi-walled carbon nanotubes, surface treated with β-nucleators: namely, the amount of β phase decreased by increasing filler content.[7] Investigation of iPP/Kevlar fiber composites revealed the strong α-nucleating ability of these fibers and the presence of a transcrystalline layer on their surface. However, for β-nucleated iPP/Kevlar fiber composites, the dominant modification was the β-form, and their crystallization characteristics were independent of the addition of Kevlar

fibers, indicating that the α-nucleating effect of Kevlar fibers was masked by the β-nucleating effect of the β-nucleator.[46]

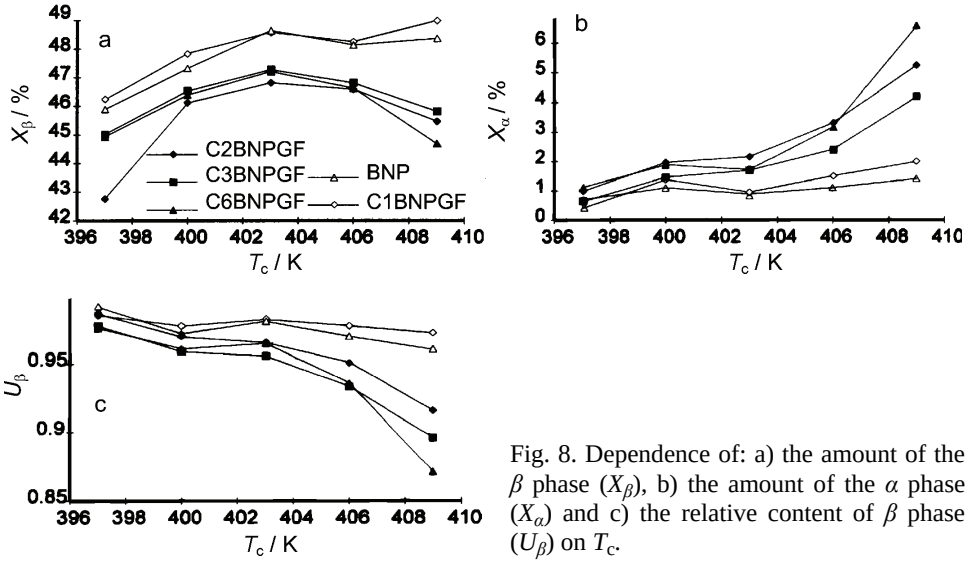

Fig. 8. Dependence of: a) the amount of the β phase (X_β), b) the amount of the α phase (X_α) and c) the relative content of β phase (U_β) on T_c.

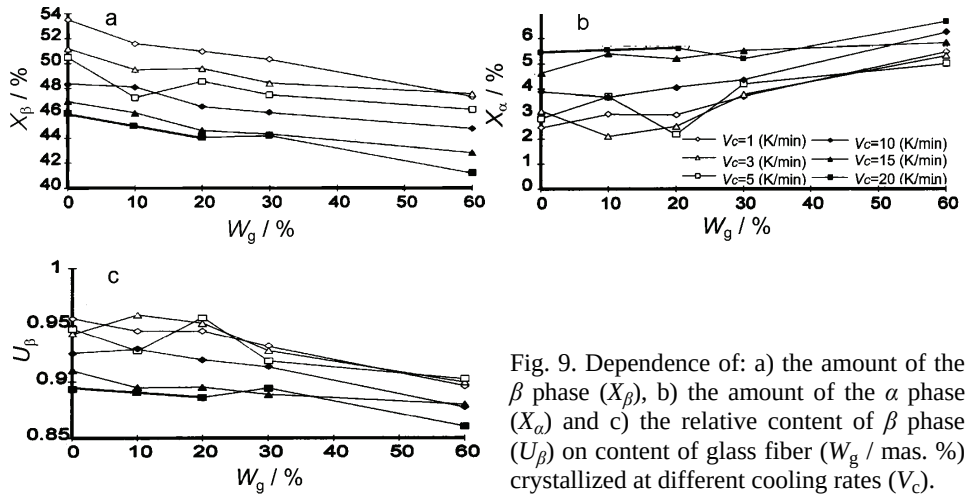

Fig. 9. Dependence of: a) the amount of the β phase (X_β), b) the amount of the α phase (X_α) and c) the relative content of β phase (U_β) on content of glass fiber (W_g / mas. %) crystallized at different cooling rates (V_c).

It could be concluded that the increased T_m^0 and σ_e observed for some model composites resulted from the increased content of α-phase. This is in agreement with the findings of Varga[41] that the variations in the results for the thermodynamic and kinetics parameters for β-iPP are most probably due to the presence of different amounts of α-phase in the examined samples.

The results of nonisothermal crystallization showed that heterogeneous nucleation activity is predominant in the model composites, even at low glass

fiber contents. The nucleation activity during the crystallization of the polymer melt was evaluated by the Dobreva method,[45] which enables the determination of the work of heterogeneous and homogeneous nucleation in polymer systems with different additives/substrates by calculating the θ-parameter. For an extremely active substrate $\theta = 0$ and for an inert substrate $\theta = 1$.

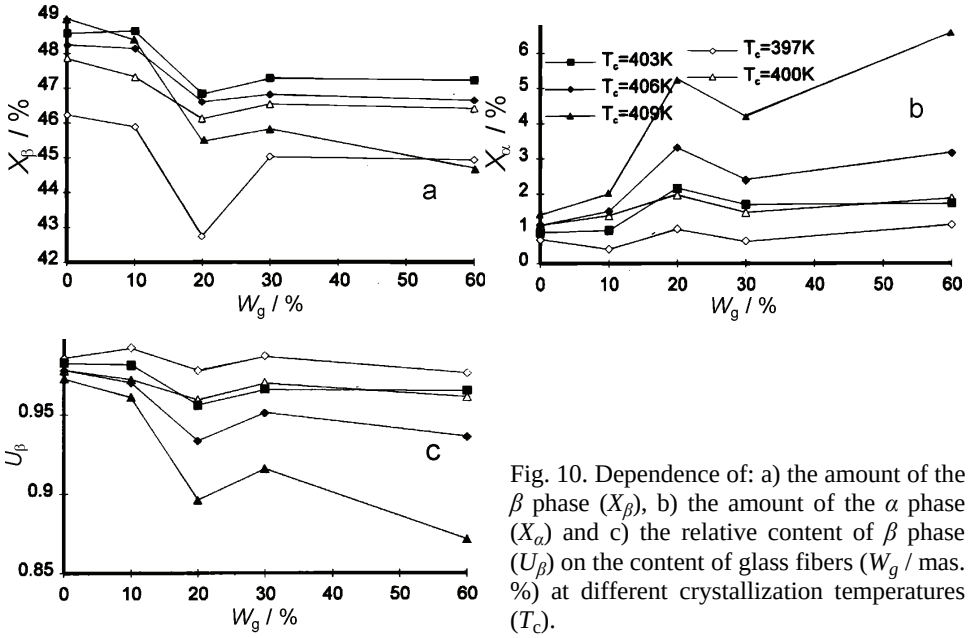

Fig. 10. Dependence of: a) the amount of the β phase (X_β), b) the amount of the α phase (X_α) and c) the relative content of β phase (U_β) on the content of glass fibers (W_g / mas. %) at different crystallization temperatures (T_c).

The results for θ-parameter are collected in Table II. For BNP, $\theta = 0.34$, and this low value was expected, since all the β-phase ($U_\beta = 0.95$ for $V_c = 1$ K min^{-1} and $U_\beta = 0.90$ for $V_c = 20$ K min^{-1}) originated from heterogeneous nucleation. In GF-model composites, the heterogeneous nucleation was obviously depressed to some level by the presence of the fibers and the θ-parameter reached higher values, 0.43–0.46.

The appearance of the α-phase in the model composites was obviously a consequence of the presence of the glass fibers (Fig. 9). In a previous investigation, it was shown that the glass fibers influenced the stability of the α-crystalline phase in glass fiber/iPP composites.[26] Their presence in BNP composites resulted in a similar effect, namely they induced the formation of certain amounts of the α-crystalline phase.

DSC melting traces of the non-isothermally crystallized C6BNPGF sample and BNP are shown in Fig. 11: similarly to the existence of two α phases in iPP (α_1 and α_2 crystalline modifications, susceptible to recrystallization), there appeared two melting peaks characteristic for the corresponding β phases of iPP.[41]

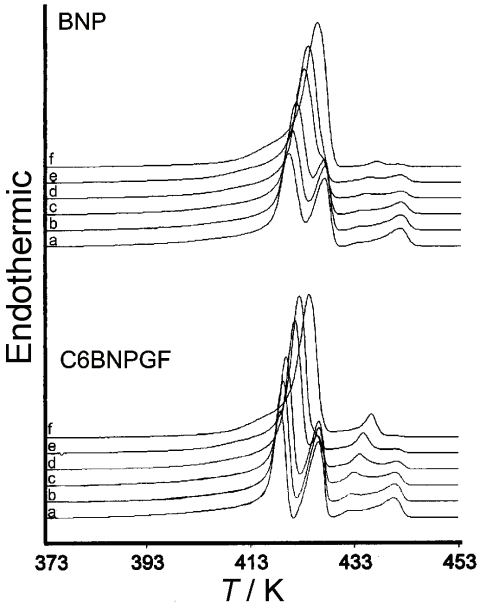

Fig. 11. Heating thermograms of BNP and C6BNPGF crystallized at different cooling rates (V_c): a) 20, b) 15, c) 10, d) 5, e) 3 and f) 1 K min^{-1}.

As a measure of the stability of the β crystal structure, the difference between the maximum of the high and low-melting peaks, ΔT_{mp} were used,[26] which are a consequence of the melting and recrystallization processes of the β_1 and β_2 crystalline modifications.[14] The dependences of ΔT_{mp} on the cooling rate, crystallization peak temperature and glass fiber content are shown in Fig. 12. As could be seen, the presence of glass fibers and their content influences the stability of the β-crystalline phase and this effect becomes more evident at $V_c \geq 3$ K min^{-1}.

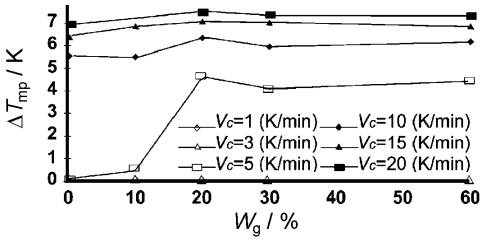

Fig. 12. Dependence of the difference between the maximum of the high and low-melting peaks (ΔT_{mp}) on content of glass fibers crystallized at different cooling rates (V_c).

CONCLUSIONS

Glass fibers, as weak α-nucleators for iPP, had an insignificant effect on the morphology of β-nucleated iPP in glass fiber composites. The thermodynamic and kinetics parameters of crystallization of BNP in the model composites were similar to those obtained for the nucleated polymer. The relative content of β-crystalline phase decreased only by several percents on increasing the content

of glass fibers from 10 to 60 mas. %, due to the appearance of α-crystallites. The relative content of β-phase depended mostly on the crystallization conditions; the lowest value of U_β (for the highest fiber content) was 0.85. The combination of excellent mechanical properties of glass fibers and the high content of the stable β-phase structure of BNP makes this system appropriate for the development of BNP/glass fiber composites with a good balance of strength and toughness.

SUPPLEMENTARY MATERIAL

Theoretical background of the approach applied is available electronically from http://www.shd.org.rs/JSCS/, or from the corresponding author on request.

ИЗВОД

УТИЦАЈ СТАКЛЕНИХ ВЛАКАНА НА МОРФОЛОГИЈУ β-НУКЛЕИСАНОГ iPP АНАЛИЗИРАН ПОМОЋУ DSC

ACO JANEVSKI[1] и GORDANA BOGOEVA-GACEVA[2]

[1]*Faculty for Technology, Goce Delcev University, 2000 Štip, Macedonia и* [2] *Faculty of Technology and Metallurgy, St. Cyril and Methodius University, 1000 Skopje, FYR Macedonia*

Присуство пуниоца и влакана значајно утиче на морфологију семикристалних полимера. Утицај стаклених влакана на морфологију β-нуклеисаног изотактичног поли(припилена) (iPP) формираног током изотермске или неизотермске кристализације, праћен је DSC анализом, а кинетички и термодинамички параметри кристализације су одређени за композите са садржајем стаклених влакана 10–60 mas. %. Присуство стаклених влакана у модел композиту са β-iPP незнатано утиче на морфологију полимерне матрице. Термодинамички и кинетички параметри кристализације i-PP у модел композиту су веома слични добијеним са β-нуклеисаним полимером. Са порастом садржаја стаклених влакана од 10 do 60 mas. % незнатно је промењен и релативни садржај β-кристалне фазе као последица појаве α-кристалита. Међутим, стабилност β-кристалне фазе се смањује са повећањем садржаја стаклених влакана и појаве β_1 и β_2 фаза, које су познате по томе што лако подлежу рекристализацији.

(Примљено 23 марта, ревидирано 26. маја, прихваћено 27. маја 2014)

REFERENCES

1. J. G. Jiang, G. Li, H. Liu, Q. Ding, K. Mai, *Composites, A* **45** (2013) 88
2. T. Bàràny, A. Izer, J. Karger-Kocsis, *Polym. Test.* **28** (2009) 176
3. Q. Ding, Z. Zhanga, C. Wanga, J. Jiang, G. Li, K. Mai, *Thermochim. Acta* **536** (2012) 47
4. J. Jiang, G. Li, N. Tan, Q. Ding, K. Mai, *Thermochim. Acta* **546** (2012) 127
5. Q. Ding, Z. Zhang, C. Wang, J. Jiang, G. Li, K. Mai, *Polym. Bull.* **70** (2013) 919
6. S. Wang, W. Yang, R. Bao, B. Wang, B. Xie, M. Yang, *Colloid Polym. Sci.* **288** (2010) 681
7. N. Zhang, Q. Zhang, K. Wang, H. Deng, Q. Fu, *J. Therm. Anal. Calorim.* **107** (2012) 733
8. A. Menyhàrd, G. Dora, Z. Horvàth, G. Faludi, J. Varga, *J. Therm. Anal. Calorim.* **108** (2012) 613
9. L. Xu, X. Zhang, L. Zhu, X. Lian, K. Xu, M. Chen, *J. Macromol. Sci., B* **50** (2011) 89
10. J. Menczel, J. Varga, *J. Therm. Anal.* **28** (1983) 161
11. C. Grein, *Adv. Polym. Sci.* **188** (2005) 93

12. R. Cermak, M. Obadal, P. Ponizil, M. Polaskova, K. Stoklasa, A. Lengalova, *Eur. Polym. J.* **41** (2006) 1836
13. J. Kotek, M. Raab, J. Baldrian, W. Grellmann, *J. Appl. Polym. Sci*. **85** (2002) 1174–1184.
14. J. Varga, *J. Macromol. Sci. Phys*. **41** (2002) 1121
15. H. B. Chen, J. Karger-Kocsis, J. S. Wu, J. Varga, *Polymer* **43** (2002) 6505
16. R. Cermak, M. Obadal, P. Ponizil, M. Polaskova, K. Stoklasa, A. Lengalova, *Eur. Polym. J.* **42** (2006) 2185
17. C. Grein, G. Plummer, H. Kausch, Y. Germain, P. Beguelin, *Polymer* **43** (2002) 3279
18. M. Fujiyama, *Int. Polym. Proc.* **10** (1995) 172
19. S. Brückner, V. Meille, V. Petraccone, B. Pirozzi, *Prog. Polym. Sci*. **16** (1991), 361
20. B. Lotz, J. C. Wittmann, A. J. Lovinger, *Polymer* **37** (1996) 4979
21. J. Varga, in *Polypropylene: Structure, Blends and Composites*, Vol. 1, *Structure and Morphology*, J. Karger-Kocsis, Ed., Chapman & Hall, London,1995, p. 56
22. A. Zeng, Y. Zheng, Y. Guo, S. Qiu, L. Cheng, *Mater. Design* **34** (2012) 691
23. M. R. Meng, Q. Dou, *J. Macromol. Sci. B* **48** (2009) 213
24. G. Bogoeva-Gaceva, A. Janevski, E. Mader, *Polymer* **42** (2001) 4409
25. G. Bogoeva-Gaceva, A. Janevski, E. Mader, E. *J. Adhes. Sci. Technol.* **14** (2000) 363
26. A. Janevski, G. Bogoeva-Gaceva, E. Mader, *J. Appl. Polym. Sci*. **74** (1999) 239
27. A. Janevski, G. Bogoeva-Gaceva, *J. Appl. Polym. Sci.* **69** (1998) 381
28. G. Bogoeva-Gaceva, A. Janevski, A. Grozdanov, *J. Appl. Polym. Sci*. **67** (1988) 395
29. G. Shi, B. Huang, J. Zhang, *Makromol. Chem.-Rapid Commun.* **5** (1984) 573
30. M. Avella, E. Martuscelli, C. Sellit, E. Garagnani, *J. Mater. Sci.* **22** (1987) 3185
31. B. Monasse, J. M. Haudin, *Colloid Polym. Sci*. **264 (**1986) 117
32. S. Brandup, and E. H. Imergut, , *Polymer Handbook*, Interscience, New York, 1975, p. 24
33. M. Liu, B. Guo, M. Du, F. Chen, D. Jia, *Polymer* **50** (2009) 3022
34. J. Varga, F. Schulec-Toth, M. Pati, (J. Varga), Hungarian Patent Application, P92 01422, 1992
35. A. Turner-Jones, J. M. Aizlewod, D. R. Beckett, *Makromolekul. Chem.* **75** (1964) 134
36. G. Shi, X. Zhang, Z. Qui, *Makromolekul. Chem.* **193** (1992) 583
37. J. Garbarczuk, *Makromolekul. Chem.* **186** (1985) 2145
38. J. Varga, Y. Fujiwara, A. Ille, *Periodica Polytech. Chem. Eng.* **34** (1990) 255
39. J. Varga, in *Polypropylene: Structure, Blends and Composites*, Vol. 1, *Structure and Morphology*, J. Karger-Kocsis, Ed., Chapman & Hall, London, 1995, p. 80
40. J. D. Hoffman, *Soc. Plast. Eng. Trans.* **4** (1964) 315
41. J. Varga, I. Mudra, G. Ehrenstein, *J. Appl. Polym. Sci*. **74** (1990) 2357
42. J. Duan, Q. Dou, *J. Appl. Polym. Sci*. **130** (2013) , 206
43. R. Zhang, R. K. Y. Li, *Polym. Int*. **62** (2013) 919
44. Z. Zhao, Z. Cai, Z. Xin, *Polymer* **49** (2008) 2745
45. V. Dobreva, I. Gutzov, *Cryst. Res. Technol.* **25** (1990) 927
46. Y. Cao, J. Feng, P. Wu, *J. Therm. Anal. Calorim.* **103** (2011) 339.